

First detection of doubly deuterated methyl acetylene (CHD₂CCH and CH₂DCCD)[★]

M. Agúndez¹, E. Roueff², C. Cabezas¹, J. Cernicharo¹, and N. Marcelino¹

¹ Instituto de Física Fundamental, CSIC, C/ Serrano 123, E-28006 Madrid, Spain
e-mail: marcelino.agundez@csic.es

² LERMA, Observatoire de Paris, PSL Research University, CNRS, Sorbonne Université, F-92190, Meudon, France

Received; accepted

ABSTRACT

We report the first detection in space of the two doubly deuterated isotopologues of methyl acetylene. The species CHD₂CCH and CH₂DCCD were identified in the dense core L483 through nine and eight, respectively, rotational lines in the 72-116 GHz range using the IRAM 30m telescope. The astronomical frequencies observed here were combined with laboratory frequencies from the literature measured in the 29-47 GHz range to derive more accurate spectroscopic parameters for the two isotopologues. We derive beam-averaged column densities of $(2.7 \pm 0.5) \times 10^{12} \text{ cm}^{-2}$ for CHD₂CCH and $(2.2 \pm 0.4) \times 10^{12} \text{ cm}^{-2}$ for CH₂DCCD, which translate to abundance ratios $\text{CH}_3\text{CCH}/\text{CHD}_2\text{CCH} = 34 \pm 10$ and $\text{CH}_3\text{CCH}/\text{CH}_2\text{DCCD} = 42 \pm 13$. The doubly deuterated isotopologues of methyl acetylene are only a few times less abundant than the singly deuterated ones, concretely around 2.4 times less abundant than CH₃CCD. The abundances of the different deuterated isotopologues with respect to CH₃CCH are reasonably accounted for by a gas-phase chemical model in which deuteration occurs from the precursor ions C₃H₆D⁺ and C₃H₅D⁺, when the ortho-to-para ratio of molecular hydrogen is sufficiently low. This points to gas-phase chemical reactions, rather than grain-surface processes, as responsible for the formation and deuterium fractionation of CH₃CCH in L483. The abundance ratios $\text{CH}_2\text{DCCH}/\text{CH}_3\text{CCD} = 3.0 \pm 0.9$ and $\text{CHD}_2\text{CCH}/\text{CH}_2\text{DCCD} = 1.25 \pm 0.37$ observed in L483 are consistent with the statistically expected values of three and one, respectively, with the slight overabundance of CHD₂CCH compared to CH₂DCCD being well explained by the chemical model.

Key words. astrochemistry – line: identification – molecular processes – ISM: molecules – radio lines: ISM

1. Introduction

Deuterium fractionation is an extraordinary tool to study the early stages of star formation, in particular, the pre-stellar core phase, where the cold temperatures and high CO depletion offer optimal conditions to enrich molecules in deuterium, and the protostellar Class 0 phase, where the gas displays some of the largest levels of deuteration observed as a consequence of the inheritance of gas and ice molecules enriched in deuterium during the pre-stellar core phase (Ceccarelli et al. 2014). The cosmic D/H ratio is 1.5×10^{-5} (Linsky 2003), but deuterium fractionation is so efficient in these environments that deuterated molecules can reach abundances as high as 30-40 % relative to the parent hydrogenated species, as occurs for HDCS (Marcelino et al. 2005) and CH₂DOH (Parise et al. 2006). Moreover, for abundant molecules containing more than one hydrogen atom, multiply deuterated forms have been observed with abundance enhancements of many orders of magnitude over the statistically expected value.

Molecules with two deuterium atoms observed to date comprise D₂CO (Turner 1990; Ceccarelli et al. 1998), NHD₂ (Roueff et al. 2000), CHD₂OH (Parise et al. 2002), D₂S (Vastel et al. 2003), D₂H⁺ (Vastel et al. 2004; Parise et al. 2011), D₂CS (Marcelino et al. 2005), D₂O (Butner et al. 2007), *c*-C₃D₂ (Spezzano et al. 2013), CHD₂CN (Calcutt et al. 2018), HCOOCHD₂ (Manigand et al. 2019), and ND₂ (Melosso et al. 2020; Bac-

mann et al. 2020). Even a couple of triply deuterated molecules have been detected: ND₃ (Lis et al. 2002; van der Tak et al. 2002; Roueff et al. 2005) and CD₃OH (Parise et al. 2004). Multiply deuterated molecules have abundances relative to the hydrogenated species ranging from 5×10^{-5} , in the case of D₂O for hot corino conditions (Butner et al. 2007), to values of the order of 10 % in cold dark cloud environments, which may become comparable to those of the corresponding singly deuterated species, as occurs for D₂CS (Marcelino et al. 2005; Vastel et al. 2018; Agúndez et al. 2019) and D₂CO (Parise et al. 2006). It is remarkable that in the case of the ion H₃⁺, whose deuterated species drive most of the deuterium fractionation in the gas phase, the doubly deuterated form (first detected unambiguously by Parise et al. 2011) has an abundance similar to that of the singly deuterated species. Moreover, chemical models predict that the different deuterated species H₂D⁺, D₂H⁺, and D₃⁺ become occasionally more abundant than H₃⁺ itself for some time intervals and specific physical conditions (Roberts et al. 2004; Sipilä et al. 2017).

Multiply deuterated molecules allow to put constraints on the deuteration mechanism, either in the gas phase or in the surface of dust grains, and by extension on the formation process of the precursor hydrogenated molecule. If deuterium fractionation occurs in the gas phase, the resulting abundance ratios between singly, doubly, and even triply deuterated forms of a given molecule vary depending on the abundances of H₂D⁺, D₂H⁺, and D₃⁺ and the efficiency of the reactions of deuterium transfer from these ions, which in turn depend on parameters like the gas kinetic temperature, the level of CO depletion, and the ortho-to-

[★] Based on observations carried out with the IRAM 30m Telescope. IRAM is supported by INSU/CNRS (France), MPG (Germany) and IGN (Spain).

Table 1. Observed line parameters of CHD₂CCH and CH₂DCCD in L483.

Transition	Frequency (MHz)	$\Delta\nu$ (km s ⁻¹)	T_A^* peak (mK)	$\int T_A^* dv$ (mK km s ⁻¹)
CHD ₂ CCH				
5 _{1,5} -4 _{1,4}	76643.616	0.47(6)	12.9	6.5(6)
5 _{0,5} -4 _{0,4}	76979.250	0.37(4)	33.0	13.1(11)
5 _{1,4} -4 _{1,3}	77317.279	0.42(5)	21.5	9.7(11)
6 _{1,6} -5 _{1,5}	91971.307	0.29(4)	17.4	5.3(8)
6 _{0,6} -5 _{0,5}	92372.787	0.27(2)	31.0	8.9(7)
6 _{1,5} -5 _{1,4}	92779.672	0.30(6)	17.4	5.6(9)
7 _{1,7} -6 _{1,6}	107298.386	0.30(6)	13.7	4.4(7)
7 _{0,7} -6 _{0,6}	107765.046	0.29(3)	28.3	8.7(9)
7 _{1,6} -6 _{1,5}	108241.467	0.39(7)	15.5	6.5(9)
CH ₂ DCCD				
5 _{1,5} -4 _{1,4}	73589.402	0.31(5)	12.5	4.2(7)
5 _{0,5} -4 _{0,4}	73861.275	0.35(5)	24.8	9.1(13)
5 _{1,4} -4 _{1,3}	74133.292	0.36(10)	11.4	4.4(11)
6 _{1,6} -5 _{1,5}	88306.511	0.42(9)	12.0	5.4(9)
6 _{1,5} -5 _{1,4}	88959.161	0.36(8)	15.3	5.9(9)
7 _{1,7} -6 _{1,6}	103023.214	0.35(6)	11.4	4.2(6)
7 _{0,7} -6 _{0,6}	103402.198	0.34(3)	23.6	8.5(6)
7 _{1,6} -6 _{1,5}	103784.607	0.41(9)	8.9	3.9(6)

Numbers in parentheses are 1σ uncertainties in units of the last digits. Line parameters were derived from a Gaussian fit to the line profile. Observed frequencies are obtained adopting $V_{\text{LSR}} = 5.30 \text{ km s}^{-1}$ (Agúndez et al. 2019) and have an uncertainty of 20 kHz for all the lines. $\Delta\nu$ is the full width at half maximum.

para ratio of H₂ (Roberts et al. 2004; Roueff et al. 2005; Flower et al. 2006). If deuteration occurs on grains surfaces, the relative abundances of the different deuterated forms of a molecule are expected to follow a statistical pattern as they should basically depend on the relative arrival rates on grains of D and H atoms from the gas phase and thus on the abundance ratio between atomic D and H in the gas phase (Brown & Millar 1989).

For molecules with various hydrogen atoms among which some of them are equivalent, the relative abundances of the different deuterated variants can also give clues on the formation of the molecule. For example, for methanol (CH₃OH) deuteration on the methyl group is three times more probable than on the hydroxyl group, but observed CH₂DOH/CH₃OD ratios differ significantly from the statistical value of three, with values well above or below depending on the source (Parise et al. 2006; Ratajczak et al. 2011; Agúndez et al. 2019). The case of methyl acetylene (CH₃CCH) is also interesting as, similarly to methanol, it contains a methyl group with three equivalent H atoms and one non-equivalent H atom in the terminal CCH group. The two singly deuterated forms of CH₃CCH, CH₂DCCH and CH₃CCD, were first detected in the interstellar medium by Gerin et al. (1992) and Markwick et al. (2005), respectively. Using the ARO 12m telescope, Markwick et al. (2005) reported CH₂DCCH/CH₃CCD ratios in the range 1.20-2.04 along the TMC-1 ridge, significantly different from the statistical value of three, although in L483 the observed ratio is consistent with the statistical value (Agúndez et al. 2019).

Here we report the first identification in space of the two forms of doubly deuterated methyl acetylene: CHD₂CCH and CH₂DCCD. These species were detected toward the dense core L483 using the IRAM 30m telescope. The observation of the two singly and two doubly deuterated forms of methyl acetylene stimulated us to build a gas-phase chemical model, including multiply deuterated species, to investigate the mechanisms of deuteration of CH₃CCH in L483.

2. Observations

The target of the observations, L483, is a dark cloud core located in the Aquila Rift star-forming region, which hosts an embedded infrared source, IRAS 18148–0440, classified as a Class 0 object. The observations were carried out with the IRAM 30m telescope in the frame of a λ 3 mm line survey covering the 80-116 GHz range (Agúndez et al. 2019). Additional observations in the 72-80 GHz range were taken with the IRAM 30m telescope in December 2018. During this observing run, weather conditions were good, with 4-5 mm of precipitable water vapor.

We describe briefly the observations. For more details we refer to Agúndez et al. (2019). We used the EMIR receiver E090 connected to a fast Fourier transform spectrometer providing a spectral resolution of 50 kHz. All observations were carried out using the frequency-switching technique, with a frequency throw of 7.2 MHz. Intensities are expressed in terms of T_A^* , the antenna temperature corrected for atmospheric absorption and for antenna ohmic and spillover losses. The uncertainty in T_A^* is estimated to be 10 %. The antenna temperature T_A^* can be converted to main beam brightness temperature T_{mb} by dividing by $B_{\text{eff}}/F_{\text{eff}}$, where $B_{\text{eff}} = 0.871 \exp[-(\nu(\text{GHz})/359)^2]$ and $F_{\text{eff}} = 0.95^1$. Pointing errors were typically 2-3'' and the half power beam width of the IRAM 30m telescope ranges between 34'' at 72 GHz and 21'' at 116 GHz. All data were reduced using the program CLASS of the GILDAS software package².

3. Results

3.1. Detection of CHD₂CCH and CH₂DCCD in L483

In the data of L483 covering the 72-116 GHz frequency range there are several lines which could not be assigned to any known molecule after inspection of the CDMS³ (Müller et al. 2005) and JPL⁴ (Pickett et al. 1998) catalogues. Several of these unidentified lines could be grouped in sets of three lines with harmonic relations 5/6/7, with rotational constants around either 7700 MHz or 7400 MHz. These values are close to the rotational constants B or $(B + C)/2$ of the isotopologues of methyl acetylene. For example, for CH₃CCD the rotational constant B is 7788 MHz and for CH₂DCCH the value of $(B + C)/2$ is 8091 MHz (Le Guennec et al. 1993). A closer inspection of the private catalogue of J. Cernicharo generated from the MADEX code⁵ (Cernicharo 2012) revealed that the observed frequencies of these sets of harmonically related lines differ by 0.9-2.7 MHz and 0.2-1.7 MHz from the frequencies predicted for rotational transitions of CHD₂CCH and CH₂DCCD, respectively. The rotational spectrum of these two molecules has been measured in the laboratory in the frequency range 29-47 GHz with uncertainties of 0.1 MHz in the frequencies (Thomas et al. 1955). Using these data, the frequencies predicted for the 72-116 GHz range have errors of a few MHz, and this is the reason why some of the unidentified lines seen in the 80-116 GHz range were not properly assigned to CHD₂CCH and CH₂DCCD by Agúndez et al. (2019). In fact, the identification of these two molecules reduces drastically the number of lines pending of identification in the λ 3 mm line survey of L483 (see Table A.2 of Agúndez et al. 2019). The parameters derived for the lines assigned to the two doubly deuterated isotopologues of methyl acetylene are given in Table 1 and the

¹ <http://www.iram.es/IRAMES/mainWiki/Iram30mEfficiencies>

² <http://www.iram.fr/IRAMFR/GILDAS>

³ <https://cdms.astro.uni-koeln.de/>

⁴ <https://spec.jpl.nasa.gov/>

⁵ https://nanocosmos.iff.csic.es/?page_id=1619

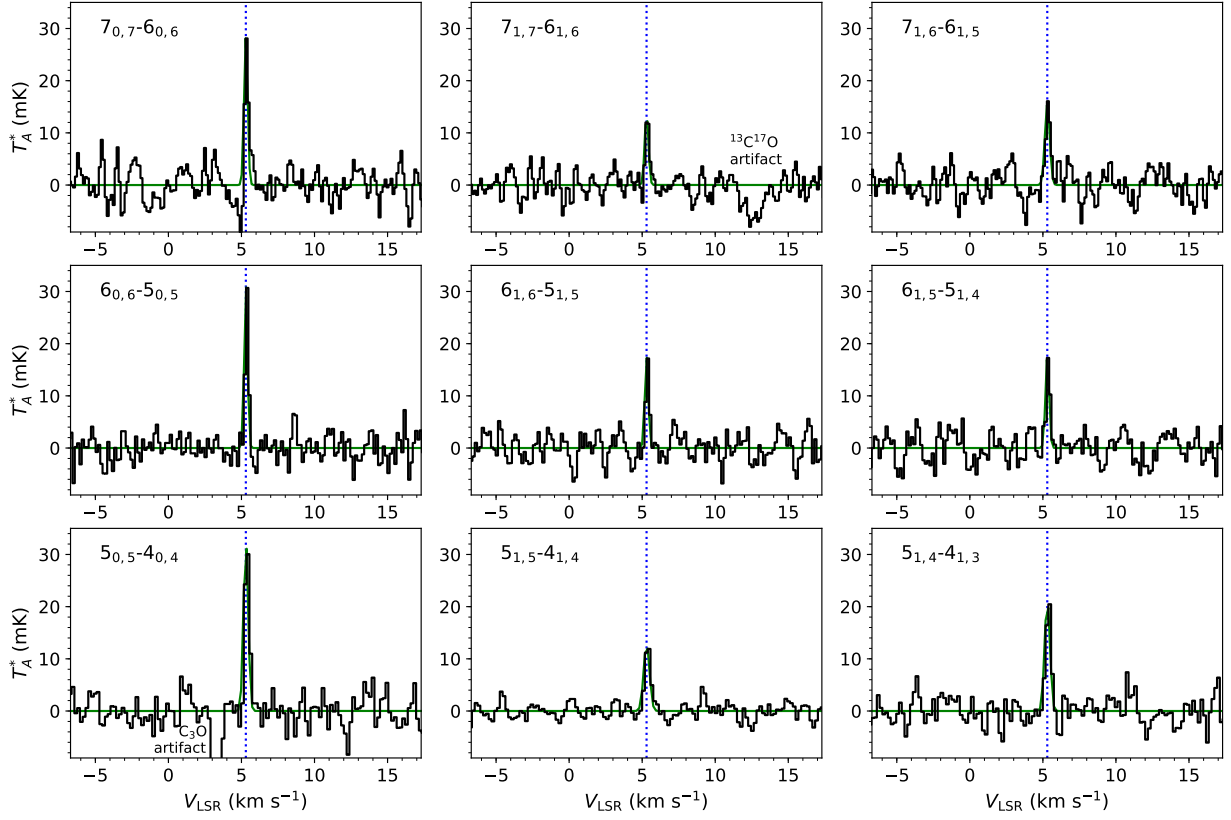


Fig. 1. Observed lines of CHD₂CCH in L483 in the 72-116 GHz range. The systemic velocity of L483 (5.30 km s⁻¹) is indicated by a vertical dotted blue line. Green lines are Gaussian fits to each line profile. Frequencies and line parameters are given in Table 1.

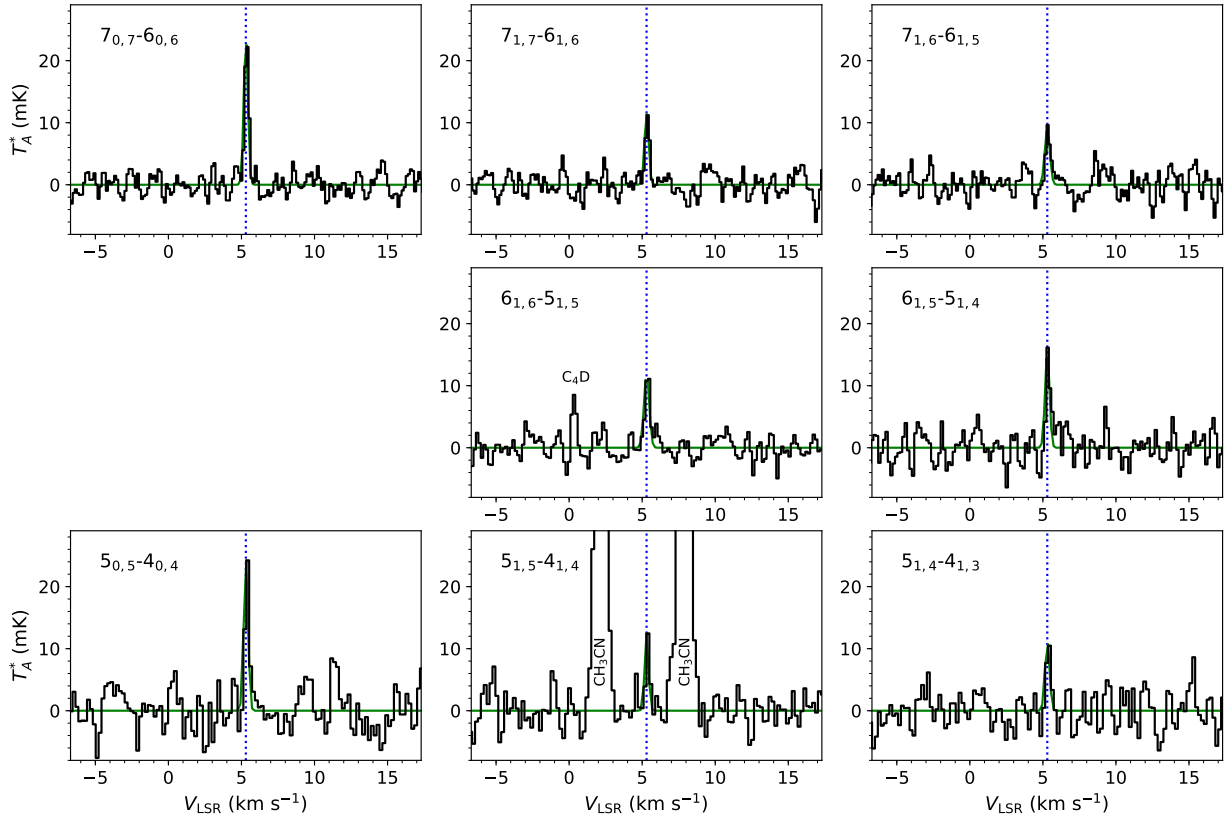


Fig. 2. Observed lines of CH₂DCCD in L483 in the 72-116 GHz range. The systemic velocity of L483 (5.30 km s⁻¹) is indicated by a vertical dotted blue line. Green lines are Gaussian fits to each line profile. Frequencies and line parameters are given in Table 1. The 6_{0,6}-5_{0,5} line is not detected because it overlaps with the strong HCN $J = 1-0$ line.

Table 2. Spectroscopic parameters of CHD₂CCH and CH₂DCCD.

Parameter	CHD ₂ CCH	CH ₂ DCCD
A_0 (MHz)	95746(533)	119688.0(170)
B_0 (MHz)	7765.71927(255)	7440.77759(341)
C_0 (MHz)	7630.99013(254)	7332.00345(340)
Δ_J (kHz)	2.3807(270)	2.0759(347)
Δ_{JK} (kHz)	123.83(224)	118.93(295)
N^a	16	17
rms (kHz) ^b	52	80

Numbers in parentheses are 1σ uncertainties in units of the last digits.

^a Number of lines included in the fit. For CHD₂CCH, $J_{\max} = 7$, $K_{\max} = 2$, and $\nu_{\max} = 108.241$ GHz, and for CH₂DCCD, $J_{\max} = 7$, $K_{\max} = 2$, and $\nu_{\max} = 103.784$ GHz. ^b Root mean square of the fit.

observed line profiles are shown in Fig. 1 for CHD₂CCH and in Fig. 2 for CH₂DCCD. We note that the line at 91971.307 MHz, assigned to the $6_{1,6}-5_{1,5}$ transition of CHD₂CCH, was incorrectly assigned to the transition 5_3-4_3 $F = 6-5$ of CH₃CN by Agúndez et al. (2019).

The astronomical frequencies observed in the 72-116 GHz range (see Table 1) and the laboratory frequencies measured in the 29-47 GHz range (Thomas et al. 1955) were used to derive more accurate spectroscopic parameters for CHD₂CCH and CH₂DCCD (see Table 2). These constants improve considerably over those reported by Thomas et al. (1955) and allow to predict the rotational spectrum of the two molecules with an accuracy better than 0.1 MHz up to 200 GHz. Since the lines of doubly deuterated CH₃CCH are relatively bright in L483, it would not be surprising to detect the triply deuterated species CHD₂CCD, which should be three times more abundant than CD₃CCH. However, the rotational spectrum has only been measured in the 28-43 GHz range with a modest accuracy (Thomas et al. 1955), which may translate to frequency errors of a few MHz for lines lying above 72 GHz. It would therefore be interesting to measure the rotational spectrum of triply deuterated CH₃CCH at millimeter wavelengths.

3.2. Observed column densities

We derived beam-averaged column densities for methyl acetylene and its singly and doubly deuterated isotopologues in L483 assuming local thermodynamic equilibrium. Values for CH₃CCH and the two singly deuterated forms were already reported by Agúndez et al. (2019). Here we have revised some of these values including new lines observed in the 72-80 GHz range and using new values for the electric dipole moments.

The dipole moment of CH₃CCH was experimentally measured by Burrell et al. (1980) to be 0.7839 D. For CH₃CCD, the dipole moment was measured by Muentert & Laurie (1966). Here we adopt the value measured by these latter authors cor-

rected by using a more accurate value of the dipole moment of OCS, which is used as reference (see Burrell et al. 1980). The dipole moment of CH₃CCD turns out to be only $\sim 2\%$ lower than that of CH₃CCH (see Table 3). For CH₂DCCH, CHD₂CCH, and CH₂DCCD, all of which are asymmetric rotors, dipole moments are not known, and we thus evaluated them using quantum chemical calculations. Since for these species the dipole moment is only due to vibrational effects connected to isotopic substitution, anharmonic force field calculations were required. All the calculations were done using the orbital-dependent functional (dubbed B2PLYP) (Grimme 2006) with the Becke-Johnson D3(BJ) damping function (Risthaus & Grimme 2013) and the Dunning's basis set cc-pVTZ (Dunning 1989). In order to obtain more reliable values we also calculated the dipole moments for CH₃CCH, CD₃CCH, CH₃CCD and CD₃CCD, whose dipole moments are experimentally known (Muentert & Laurie 1966; Burrell et al. 1980). In this manner, we obtained an experimental/theoretical ratio that was used to correct the theoretical values for CH₂DCCH, CHD₂CCH, and CH₂DCCD. The calculated dipole moments along the principal axis a , which is the relevant parameter since the observed lines are of a -type, are given in Table 3. It is found that they differ only slightly, up to $\sim 2\%$, from that of CH₃CCH.

For CH₃CCD we now include two new lines, the 5_0-4_0 and 5_1-4_1 , observed in the 72-80 GHz range. For CH₃CCH, we observed lines with $K = 0, 1, 2, 3$, and thus the column density includes these four K ladders, although the $K = 0$ and $K = 1$ levels account for most of the column density (92 %). For CH₃CCD only $K = 0$ and $K = 1$ lines were observed. Among all isotopologues of methyl acetylene, CH₂DCCH has the most precise determination of the rotational temperature, 10.2 ± 0.7 K, due to the higher number of lines observed and the wider range of upper level energies involved. We therefore adopted this value for all other isotopologues when deriving column densities. We note that if the rotational temperature is not fixed, the values obtained are consistent with the rotational temperature of 10.2 K adopted. For example, for CHD₂CCH we obtain a rotational temperature of 9.3 ± 1.3 K while for CH₂DCCD we get 11.4 ± 2.0 K. The rotational partition function was computed by summation including energy levels up to $J = 100$. For guidance, in Table 4 we give rotational partition functions for CHD₂CCH and CH₂DCCD at different temperatures. The column densities derived in L483 for CH₃CCH and its singly and doubly deuterated forms are given in Table 3. Deuterium ratios for various molecules in L483 have been discussed by Agúndez et al. (2019). Regarding doubly deuterated methyl acetylene, the two forms show a deuterium enrichment comparable to H₂CO and H₂CS, which show the largest levels of deuteration in L483 ($H_2CO/D_2CO = 31.3$ and $H_2CS/D_2CS = 21.7$; Agúndez et al. 2019), and are significantly more enriched in deuterium than CH₃OH and c -C₃H₂, for which

Table 3. Column densities and ratios for CH₃CCH and its singly and doubly deuterated species in L483.

Species	μ (D) ^a	N_{lines} ^e	E_{up} (K) ^f	T_{rot} (K)	N (cm ⁻²) ^h	Column density ratio ⁱ	
CH ₃ CCH	0.7839 ^b	8	11.5 - 82.3	10.2 ^g	9.10×10^{13}		
CH ₂ DCCH	0.7850 ^c	15	11.6 - 43.6	10.2 ± 0.7	$(1.76 \pm 0.34) \times 10^{13}$	CH ₃ CCH / CH ₂ DCCH	5.2 ± 1.6
CH ₃ CCD	0.7698 ^d	6	10.5 - 20.9	10.2 ^g	5.79×10^{12}	CH ₃ CCH / CH ₃ CCD	15.7 ± 4.7
CHD ₂ CCH	0.7870 ^c	9	11.1 - 25.0	10.2 ^g	2.69×10^{12}	CH ₃ CCH / CHD ₂ CCH	33.8 ± 10.1
CH ₂ DCCD	0.7711 ^c	8	10.6 - 25.3	10.2 ^g	2.16×10^{12}	CH ₃ CCH / CH ₂ DCCD	42.1 ± 12.6

^a Dipole moments along the principal axis a . ^b Experimental value from Burrell et al. (1980). ^c Calculated value (this work). ^d Experimental value from Muentert & Laurie (1966) corrected for a more accurate dipole moment of the reference OCS than used by these authors (see text).

^e Number of lines observed. ^f Range of upper level energies of the lines observed. ^g Rotational temperature has been fixed to the value derived for CH₂DCCH. ^h Errors in the column densities are estimated to be 20 %. ⁱ Errors in the column density ratios are estimated to be 30 %.

Table 4. Rotational partition functions for CHD₂CCH and CH₂DCCD.

Temperature (K)	Q_{rot}^a	
	CHD ₂ CCH	CH ₂ DCCD
300.0	11646.9629	10855.0235
225.0	7563.8563	7049.8187
150.0	4117.1979	3837.5133
75.00	1456.4144	1357.4949
37.50	515.6773	480.6346
18.75	182.8944	170.4479
9.375	65.0786	60.6361
5.000	25.6362	23.8844
2.725	10.5863	9.9782

^a Computed including energy levels up to $J = 100$.

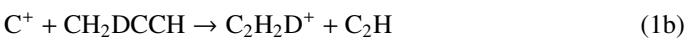
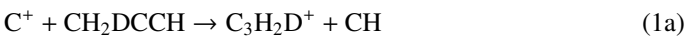
CH₃OH/CHD₂OH = 357 and c -C₃H₂/ c -C₃D₂ = 103 (Agúndez et al. 2019).

4. Chemical model

To our knowledge, detailed studies of multiple deuteration have been essentially focused on simple hydrides, like H₂O, NH₂, and NH₃ (Sipilä et al. 2015; Furuya et al. 2015; Roueff et al. 2005; Hily-Blant et al. 2018; Bacmann et al. 2020), and molecules containing a single carbon atom, like H₂CO, H₂CS, and CH₃OH (Marcelino et al. 2005; Parise et al. 2006; Taquet et al. 2012). Multiple deuteration proceeds essentially in the gas phase through successive reactions of HD with H₃⁺, H₂D⁺, and D₂H⁺, and with CH₃⁺, CH₂D⁺, and CHD₂⁺, as introduced by Roberts et al. (2004). Additional deuterium exchange reactions with HD suggested to be considered for carbon chain molecules involve C₂H₂⁺ and C₂HD⁺ (Turner 2001). We further introduce exchange reactions of C₃H⁺ with HD and D₂, which have been studied by Savić & Gerlich (2005); Savić et al. (2005) as displayed in Table 5. We estimate the endothermicity for the reverse reactions from the values reported for the cyclic and the linear isomers of C₃H and C₃D (Etim et al. 2020).

We consider here a pure gas-phase chemical network including species containing up to three deuterium atoms, extending our previous study on the recent detection of HDCCN in TMC-1 (Cabezas et al. 2021). As an example, let us mention that, in order to comply with the present observational challenges, we introduced the various isomers of deuterated methyl acetylene CH₂DCCCH, CH₃CCD, CHD₂CCH, CH₂DCCD, CD₃CCH, and CHD₂CCD. The final chemical network comprises 394 species linked through more than 14,000 reactions. When no experimental information is available, we assume that the total rate coefficient of reactions involving deuterium atoms is identical to that with hydrogenated compounds. The derivation of branching ratios is principally based on statistical considerations.

However, for deuterated methyl acetylene we consider that the external CH and CCH (or CD and CCD) groups are much more mobile than the methyl group. Then, we assume that for reactions involving the ejection of CH and CCH (or CD and CCD), only the terminal group is implied in the reaction. As an example:


Table 5. Reactions involving C₃H⁺ and C₃D⁺.

Reaction	α (cm ³ s ⁻¹)	γ (K)	Ref.
C ₃ H ⁺ + HD \rightleftharpoons C ₃ D ⁺ + H ₂	5.6×10^{-11}	500 - 375	(1)
C ₃ H ⁺ + D ₂ \rightleftharpoons C ₃ D ⁺ + HD	3.0×10^{-13}	420 - 320	(1)
C ₃ ⁺ + H ₂ \rightarrow C ₃ H ⁺ + H	1.7×10^{-9}		(1)
C ₃ ⁺ + HD \rightarrow C ₃ D ⁺ + H	9.3×10^{-10}		(1)
C ₃ ⁺ + HD \rightarrow C ₃ H ⁺ + D	7.6×10^{-10}		(1)
C ₃ ⁺ + D ₂ \rightarrow C ₃ D ⁺ + D	1.3×10^{-9}		(1)
C ₃ H ⁺ + H ₂ \rightarrow c -C ₃ H ₂ ⁺ + H	1.0×10^{-12}		(2)
C ₃ H ⁺ + HD \rightarrow c -C ₃ HD ⁺ + H	4.6×10^{-10}		(1)
C ₃ H ⁺ + HD \rightarrow c -C ₃ H ₂ ⁺ + D	3.0×10^{-12}		(1)
C ₃ H ⁺ + D ₂ \rightarrow c -C ₃ HD ⁺ + D	1.0×10^{-11}		(1)
C ₃ H ⁺ + D ₂ \rightarrow c -C ₃ D ₂ ⁺ + H	2.7×10^{-11}		(1)
C ₃ D ⁺ + H ₂ \rightarrow c -C ₃ HD ⁺ + H	1.0×10^{-12}		(3)
C ₃ D ⁺ + HD \rightarrow c -C ₃ HD ⁺ + H	1.0×10^{-10}		(1)
C ₃ D ⁺ + HD \rightarrow c -C ₃ D ₂ ⁺ + H	8.3×10^{-11}		(1)
C ₃ D ⁺ + D ₂ \rightarrow c -C ₃ D ₂ ⁺ + D	1.7×10^{-10}		(1)

The rate coefficient, α , corresponds to the value reported at 10 K or 15 K in reference (1). The first two displayed reactions correspond to deuterium exchange and γ stands for the estimated endothermicity (see text) of the reverse reaction.

References: (1) Savić & Gerlich (2005); (2) Loison et al. (2017); (3) assumed.

Table 6. Reactions involving ortho H₂.

Reaction	α (cm ³ s ⁻¹)	β	γ (K)	Ref.
o -H ₂ + H ₂ D ⁺ \rightarrow HD + H ₃ ⁺	9.4×10^{-11}	-0.79	56.0	(1)
o -H ₂ + D ₂ H ⁺ \rightarrow HD + H ₂ D ⁺	3.3×10^{-10}	-0.55	23.1	(1)
o -H ₂ + D ₂ H ⁺ \rightarrow D ₂ + H ₃ ⁺	3.5×10^{-11}	-0.82	181.7	(1)
o -H ₂ + D ₃ ⁺ \rightarrow HD + D ₂ H ⁺	9.2×10^{-10}	-0.59	68.8	(1)
o -H ₂ + D ₃ ⁺ \rightarrow D ₂ + H ₂ D ⁺	1.5×10^{-10}	-0.85	174.4	(1)
o -H ₂ + N ⁺ \rightarrow NH ⁺ + H	4.2×10^{-10}	-0.15	44.1	(2)

Reaction rate coefficient is given by $k(T) = \alpha \left(\frac{T}{300K}\right)^\beta \exp(-\gamma/T)$.

References: (1) Hily-Blant et al. (2018); (2) Dislaire et al. (2012).

For reactions of dissociative recombination, we consider that atomic hydrogen is ejected twice more efficiently than deuterium, as found in some experiments (e.g., Jensen et al. 1999). We include the findings of Savić & Gerlich (2005) and Savić et al. (2005), who showed that the rate coefficients of reactions of C₃H⁺ with HD and D₂ are different from those with H₂. We also report in Table 5 the corresponding rate coefficients used in our network. Let us point out that these values are still subject to some uncertainties as discussed in Savić & Gerlich (2005) and Savić et al. (2005).

As in our previous studies of isotopic fractionation (Roueff et al. 2015), we do not solve the full para/ortho chemistry of hydrogen compounds but rather introduce the ortho-to-para ratio of H₂, OPR, as a free parameter. This factor impacts the reverse reactions of the deuteron exchanges of HD with H₃⁺, H₂D⁺, and D₂H⁺ and the reaction N⁺ + H₂ (Dislaire et al. 2012), as shown in Table 6, where $n(o\text{-H}_2) = \frac{OPR}{1+OPR}n(\text{H}_2)$. The exponential terms, γ , were obtained by subtracting the energy of the $J = 1$ level of o -H₂, 170.5 K, from the endothermicity of the reaction with reactants and products in their ground states. We did not introduce the similar reactions CH_{3- n} D _{n} ⁺ ($n = 0, 1, 2, 3$) + o -H₂, C₂H_{2- n} D _{n} ⁺ ($n = 0, 1, 2$) + o -H₂, and C₃D⁺ + o -H₂ since the corresponding endothermicities are much larger (Roueff et al. 2013; Nyman and Yu 2019) and the reactions do not take place in the present low temperature, ~ 10 K, conditions.

Table 7 displays the deuterium ratios of various carbon-containing molecules observed in L483, including present methyl acetylene detections, and three steady-state model results

Table 7. H/D ratios of C-containing molecules observed in L483 and steady-state values calculated with our gas-phase chemical model ^a.

Molecular ratio	L483	Model 1	Model 2	Model 3
OPR H ₂		10 ⁻³	10 ⁻⁴	10 ⁻⁴
ζ (10 ⁻¹⁷ s ⁻¹) ^d		1.3	1.3	0.5
CH ₃ CCH / CH ₂ DCCD	5.2 ^c	10.1	7.6	6.3
CH ₃ CCH / CH ₃ CCD	15.7 ^c	27.3	20.4	17.1
CH ₃ CCH / CHD ₂ CCH	33.8 ^c	91.1	56.0	38.0
CH ₃ CCH / CH ₂ DCCD	42.1 ^c	131.5	78.4	54.5
<i>c</i> -C ₃ H / <i>c</i> -C ₃ D	22.7 ^d	18.2	15.4	12.8
<i>c</i> -C ₃ H ₂ / <i>c</i> -C ₃ HD	9.8 ^d	13.4	13.1	11.1
<i>c</i> -C ₃ H ₂ / <i>c</i> -C ₃ D ₂	103 ^d	173	130	95.5
<i>l</i> -C ₃ H ₂ / <i>l</i> -C ₃ HD	13.2 ^d	7.0	6.5	5.4
C ₄ H / C ₄ D	52.6 ^d	13.0	9.7	8.9
CH ₃ N / DC ₃ N	35.7 ^d	14.1	10.8	9.0
CH ₃ CN / CH ₂ DCN	7.6 ^d	18.2	15.4	13.8

^a See text for the assumed physical conditions. We adopted the elemental abundance ratios O/H = 8×10^{-6} , D/H = 1.5×10^{-5} , C/O = 0.5, and C/N = 4. ^b Cosmic-ray ionization rate of H₂. ^c Observed values in this work (see Table 3). ^d Observed values from Agúndez et al. (2019).

corresponding to the physical conditions, $n(\text{H}_2) = 3 \times 10^4 \text{ cm}^{-3}$ and $T = 10 \text{ K}$, prevailing in L483 (Agúndez et al. 2019). Model 1 represents a fiducial model with OPR = 10^{-3} and $\zeta = 1.3 \times 10^{-17} \text{ s}^{-1}$, which corresponds to typical values for dark clouds. We notice that this choice overestimates the H/D ratio of methyl acetylene by about a factor of two, a feature that we already noticed in our previous study of TMC-1 (Cabezas et al. 2021). Decreasing the ortho-to-para ratio of H₂ by a factor of ten, as done in model 2, allows to decrease reasonably the H/D ratios of the various C-containing molecules. This trend is further strengthened in model 3, where the cosmic-ray ionization rate is reduced down to $5 \times 10^{-18} \text{ s}^{-1}$, which results in H/D ratios for singly and doubly deuterated methyl acetylene close to the observed values.

While a more detailed study is highly desirable, we can make some comments. The abundance ratio between the two singly deuterated forms of methyl acetylene, CH₂DCCH/CH₃CCD, is close to three according to the observations and this fact is reproduced by the models. This feature results directly from the statistical considerations for the insertion of deuterium in the CH₃ group and in the terminal CCH group. For example, in the dissociative recombination of C₃H₆D⁺ and C₃H₅D⁺, which are the principal formation routes of deuterated methyl acetylene, we explicitly account for this statistical factor in the reaction rate coefficients. The doubly deuterated forms, on the other hand, are assumed to be produced in equal amounts from the dissociative recombinations of C₃H₅D₂⁺ and C₃H₄D₂⁺, following statistical arguments as well. The difference between the abundances of CH₂DCCD and CHD₂CCH results then from the destruction rates, for which we assume that the possible ejection of H or D occurs from the terminal CCH or CCD group. As an example, CH₂DCCD + H₃⁺ → C₃H₂D⁺ + H₂ + HD whereas CHD₂CCH + H₃⁺ → C₃HD₂⁺ + H₂ + H₂. Then, CHD₂CCH is more easily recycled in a doubly deuterated form and its abundance is somewhat larger than that of CH₂DCCD, as derived from the observations. A low ortho-to-para ratio of H₂ favors significantly the deuterium enhancement of methyl acetylene, which reflects the role of deuterium transfer in ion-molecule reactions. We note that the range 10^{-3} - 10^{-4} is within the OPR H₂ values derived for typical conditions of dark clouds (Le Boulbot 1991; Furuya et al. 2015). In a similar way, lowering the cosmic-ray ionization rate leads to a decrease in the ionization fraction, which enhances the

abundance of molecular ions and decrease the H/D ratio of the various molecular species.

We plan to further investigate the dependence of deuterium fractionation on various parameters in a dedicated study but these first results show that the gas-phase ion-molecule schema can explain the formation of methyl acetylene and its singly and doubly deuterated substitutes. Moreover, if deuteration occurs on grain surfaces and deuterated ratios are governed by the D/H ratio in the gas phase, then it would hold that CH₂DCCD/CH₃CCD = $3 \times \text{CH}_3\text{CCD}/\text{CH}_3\text{CCH}$. That is, CH₂DCCD/CH₃CCD should be 0.19, while the observed value is 0.37, meaning that doubly deuterated species are twice more abundant than expected if deuteration occurs on grain surfaces following a statistical scheme. This fact further strengthens the gas-phase origin of deuteration for methyl acetylene. It is interesting to note that our models also predict the deuteration of allene (CH₂CCH₂) at similar levels than methyl acetylene. However, the dipole moment of the fully hydrogenated form of allene is zero and that resulting from deuterium inclusion is probably too small to permit the detection of any deuterium isotopologue.

5. Conclusions

We have presented the first detection in space of the two doubly deuterated isotopologues of methyl acetylene, CHD₂CCH and CH₂DCCD, toward the dark cloud core L483. The frequencies predicted for these two species from laboratory data have significant errors when compared with those derived from astronomical observations. We have therefore derived new spectroscopic parameters for the two deuterium isotopologues which have the accuracy needed to observe these species in cold interstellar clouds showing narrow lines. We derive abundance ratios of CH₃CCH/CHD₂CCH = 34 ± 10 and CH₃CCH/CH₂DCCD = 42 ± 13 . Doubly deuterated methyl acetylene is found to be only a few times less abundant than the singly deuterated forms. We have constructed a gas-phase chemical model including multiply deuterated molecules, which is able to reproduce the abundance ratios of the different deuterated isotopologues with respect to CH₃CCH observed in L483. In particular, the fact that CHD₂CCH is slightly more abundant than CH₂DCCD is well accounted for by the chemical model. This favors a scenario in which deuteration of methyl acetylene occurs in the gas phase, rather than on the surface of dust grains.

Acknowledgements. We acknowledge funding support from Spanish MICIU through grants AYA2016-75066-C2-1-P, PID2019-106110GB-I00, and PID2019-107115GB-C21 and from the European Research Council (ERC Grant 610256: NANOCOSMOS). M.A. also acknowledges funding support from the Ramón y Cajal programme of Spanish MICIU (grant RyC-2014-16277). C.C. thanks Prof. Cristina Puzzarini (Università di Bologna) for her advices and comments about the quantum chemical calculations.

References

- Agúndez, M., Marcelino, N., Cernicharo, J. et al. 2019, A&A, 625, A147
 Bacmann, A., Faure, A., Hily-Blant, P., et al. 2020, MNRAS, 499, 1795
 Brown, P. D. & Millar, T. J. 1989, MNRAS, 1989, 240, 25
 Burrell, P. M., Bjarnov, E., & Schwendeman, R. H. 1980, J. Mol. Spectr., 82, 193
 Butner, H. M., Charnley, S. B., Ceccarelli, C., et al. 2007, ApJ, 659, L137
 Cabezas, C., Endo, Y., Roueff, E., et al. 2021, A&A, 646, L1
 Calcutt, H., Jørgensen, J. K., Müller, H. S. P., et al. 2018, A&A, 616, A90
 Ceccarelli, C., Castets, A., Loinard, L., et al. 1998, A&A, 338, L43
 Ceccarelli, C., Caselli, P., Bockelée-Morvan, D., et al. 2014, Protostars and Planets VI, 859
 Cernicharo, J. 2012, in European Conference on Laboratory Astrophysics, eds. C. Stehlé, C. Joblin, & L. d'Hendecourt, EAS Publication Series, 58, 251
 Dislaire, V., Hily-Blant, P., Maret, S., et al. 2012, A&A, 537, A20

- Dunning Jr., T. H. 1989, *J. Chem. Phys.*, 90, 1007
- Etim, E. E., Akpan, N. I., Adelagun, R. A. O., et al. 2020, *Indian J. Phys.*, doi: 10.1007/s12648-020-01747-x
- Flower, D. R., Pineau des Forêts, & Walmsley, C. M 2006, *A&A*, 449, 621
- Furuya K., Aikawa, Y., Hincelin, U., et al. 2015, *A&A*, 584, A124
- Gerin, M., Combes, F., Wlodarczak, G., et al. 1992, *A&A*, 253, L29
- Grimme, S. 2006, *J. Chem. Phys.*, 124, 034108
- Hily-Blant, P., Faure, A., Rist, C., et al. 2018, *MNRAS*, 477, 4454
- Jensen, M. J., Bilodeau, R. C., Heber, O., et al. 1999, *Phys. Rev. A*, 60, 2970
- Le Bourlot, J. 1991, *A&A*, 242, 235
- Le Guennec, M., Demaison, J., Wlodarczak, G., & Marsden, C. J. 1993, *J. Mol. Spectr.*, 160, 471
- Linsky, J. L. 2003, *Space Sci. Rev.*, 106, 49
- Lis, D. C., Roueff, E., Gerin, M., et al. 2002, *ApJ*, 571, L55
- Loison J.-C., Agúndez, M., Wakelam V., et al. 2017, *MNRAS*, 470, 4075
- Manigand, S., Calcutt, H., Jørgensen, J. K., et al. 2019, *A&A*, 623, A69
- Marcelino, N., Cernicharo, J., Roueff, E., et al. 2005, *ApJ*, 620, 308
- Markwick, A. J., Charnley, S. B., Butner, H. M., & Millar, T. J. 2005, *ApJ*, 627, L117
- Melosso, M., Bizzocchi, L., Sipilä, O., et al. 2020, *A&A*, 641, A153
- Muenter, J. S. & Laurie, V. W. 1966, *J. Chem. Phys.*, 45, 855
- Müller, H. S. P., Schlöder, F., Stutzki, J., & Winnewisser, G. 2005, *J. Mol. Struct.*, 742, 215
- Nyman, G. & Yu, H.-G. 2019, *AIP Advances* 9, 095017
- Parise, B., Ceccarelli, C., Tielens, A. G. G. M., et al. 2002, *A&A*, 393, L49
- Parise, B., Castets, A., Herbst, E., et al. 2004, *A&A*, 416, 159
- Parise, B., Ceccarelli, C., Tielens, A. G. G. M., et al. 2006, *A&A*, 453, 949
- Parise, B., Belloche, A., Du, F., et al. 2011, *A&A*, 526, A31
- Pickett, H. M., Poynter, R. L., Cohen, E. A., et al. 1998, *J. Quant. Spectr. Rad. Transfer*, 60, 883
- Ratajczak, A., Taquet, V., Kahane, C., et al. 2011, *A&A*, 528, L13
- Risthaus, T. & Grimme, S. 2013, *J. Chem. Theory Comput.*, 9, 1580
- Roberts, H., Herbst, E., & Millar, T. J. 2004, *A&A*, 424, 905
- Roueff, E., Tiné, S., Coudert, L. H., et al. 2000, *A&A*, 354, L63
- Roueff, E., Lis, D. C., van der Tak, F. F. S., et al. 2005, *A&A*, 438, 585
- Roueff, E., Gerin, M., Lis, D. C., et al. 2013, *J. Phys. Chem. A*, 117, 9959
- Roueff, E., Loison, J.-C., & Hickson, K. M. 2015, *A&A*, 576, A99
- Savić, I. & Gerlich, D. 2005, *PCCP*, 7, 1026
- Savić, I., Schlemmer, S. & Gerlich, D. 2005, *ApJ*, 621, 1163
- Sipilä, O., Harju, J., Caselli, P., & Schlemmer, S. 2015, *A&A*, 581, A122
- Sipilä, O., Harju, J., & Caselli, P. 2017, *A&A*, 607, A26
- Spezzano, S., Brünken, S., Schilke, P., et al. 2013, *ApJ*, 769, L19
- Taquet, V., Ceccarelli, C., & Kahane, C. 2012, *ApJ*, 748, L3
- Thomas, L. F., Sherrard, E. I., & Sheridan, J. 1955, *Trans. Faraday Soc.*, 51, 619
- Turner, B. E. 1990, *ApJ*, 362, L29
- Turner, B. E. 2001, *ApJS*, 136, 579
- van der Tak, F. F. S., Schilke, P., Müller, H. S. P., et al. 2002, *A&A*, 388, L53
- Vastel, C., Phillips, T. G., Ceccarelli, C., & Pearson, J. 2003, *ApJ*, 593, L97
- Vastel, C., Phillips, T. G. & Yoshida, H. 2004, *ApJ*, 606, L127
- Vastel, C., Quénard, D., Le Gal, R., et al. 2018, *MNRAS*, 478, 5514